Diagn Interv Radiol 2023; DOI: 10.4274/dir.2022.22534

BREAST IMAGING

ORIGINAL ARTICLE

Combining primary tumor features derived from conventional and contrast-enhanced ultrasound facilitates the prediction of positive axillary lymph nodes in Breast Imaging Reporting and Data System category 4 malignant breast lesions

Yu Du
Chun-Bei Yi
Li-Wen Du
Hai-Yan Gong
Li-Jun Ling
Xin-Hua Ye
Min Zong
Cui-Ying Li

Yu Du and Chun-Bei Yi have contributed equally to this study and should be considered as co-first authors.

PURPOSE

To determine whether the primary tumor features derived from conventional ultrasound (US) and contrast-enhanced US (CEUS) facilitate the prediction of positive axillary lymph nodes (ALNs) in breast cancer diagnosed as Breast Imaging Reporting and Data System (BI-RADS) category 4.

METHODS

A total of 240 women with breast cancer who underwent preoperative conventional US, strain elastography, and CEUS between September 2016 and December 2019 were included. The multiple parameters of the primary tumor were obtained, and univariate and multivariate analyses were performed to predict positive ALNs. Then three prediction models (conventional US features, CEUS features, and the combined features) were developed, and the diagnostic performance was evaluated with receiver operating characteristic curves.

RESULTS

On conventional US, the traits of large size and the non-circumscribed margin of the primary tumor were marked as two independent predictors. On CEUS, the features of vessel perforation or distortion and the enhanced range of the primary tumor were marked as two independent predictors for positive ALNs. Three prediction models were then developed: model A (conventional US features), model B (CEUS features), and model C (model A plus B). Model C yielded the highest area under the curve (AUC) of 0.82 [95% confidence interval (CI), 0.75–0.88] compared with model A (AUC 0.74; 95% CI, 0.68–0.81; $P = 0.008$) and model B (AUC 0.72; 95% CI, 0.65–0.80; $P < 0.001$) as per the DeLong test.

CONCLUSION

CEUS, as a non-invasive examination technique, can be used to predict ALN metastasis. Combining conventional US and CEUS may produce favorable predictive accuracy for positive ALNs in BI-RADS category 4 breast cancer.

KEYWORDS

Conventional ultrasound, contrast enhanced ultrasound, BI-RADS category, breast cancer, axillary lymph node metastasis

From the Department of Ultrasound (Y.D., C-B.Y., L-W.D., H-Y.G., X-H.Y., C-Y.L. ✉lcy_njmu@163.com), The First Affiliated Hospital of Nanjing Medical University, Nanjing, China; Department of Breast Surgery (L-J.L.), The First Affiliated Hospital of Nanjing Medical University, Nanjing, China; Department of Radiology (M.Z. ✉mzong@njmu.edu.cn), The First Affiliated Hospital of Nanjing Medical University, Nanjing, China.

Received 23 May 2021; revision requested 06 August 2021; last revision received 20 June 2022; accepted 30 July 2022.

Epub: 25.01.2023

Publication date: 30.05.2023

DOI: 10.4274/dir.2022.22534

Advancements in ultrasound (US) equipment have significantly increased the value of US in breast imaging. Especially in routine breast screening among women aged <50 years old, the application of US in the detection of mammographically occult masses has considerably increased.[1-3] The Breast Imaging Reporting and Data System (BI-RADS) by the American College of Radiology (ACR) is a comprehensive and normative quality control tool that was designed to standardize reporting and reduce confusion over breast imaging interpretations and management recommendations and enhance the US monitoring outcome. In 2013, the fifth edition of the BI-RADS US lexicon was published with a seven-category BI-

You may cite this article as: Du Y, Yi CB, Du LW, et al. Combining primary tumor features derived from conventional and contrast-enhanced ultrasound facilitates the prediction of positive axillary lymph nodes in Breast Imaging Reporting and Data System category 4 malignant breast lesions. *Diagn Interv Radiol.* 2023;29(3):469-477.

RADS classification system from 0 to 6, which has reinforced the standardization of breast lesion characterization with US.[4] Despite the advances in equipment and US physician experience, BI-RADS category 4 remains an issue of concern.[5] Category 4 has a wide range of malignant probabilities, from 2% to 95%,[4,6] and covers sufficiently suspicious lesions without typical malignant features, for which a biopsy is recommended. In addition, the presence or absence of regional positive lymph nodes (LN) is critical to the staging, treatment, and prognosis of breast cancer. It is considered significant to the preoperative identification of positive axillary lymph nodes (ALNs) in BI-RADS category 4 malignant lesions so as to facilitate clinical decision making on patient management.

In the past decade, the clinical use of contrast-enhanced US (CEUS) has expanded research on its application.[7,8] CEUS can provide more information about microvasculature and hemodynamics than US.[9-11] Distinguishing malignant and benign breast lesions by CEUS alone or incorporating the BI-RADS with CEUS has been extensively approved.[12] These studies demonstrate that CEUS or US+CEUS has better diagnostic performance than US alone in differentiating breast lesions, and particularly, US+CEUS has a low negative likelihood ratio.[12-15] Several studies have shown that the US characteristics of primary breast cancer are closely related to ALN metastasis and may more accurately predict the status of preoperative clinical LNs.[16-18] However, relevant literature rarely exists to report whether CEUS is useful for detecting positive ALNs in suspicious breast cancer lesions of BI-RADS category 4.

Hence, in this study, we aimed to investigate whether CEUS tumor features may help predict positive ALNs in breast cancer diagnosed as BI-RADS category 4 and probe the role of CEUS in increasing diagnostic performance.

Methods

The protocol of this study was approved by the Ethics Committee of The First Affiliated Hospital of Nanjing Medical University, and written informed consent was waived due to the retrospective nature of the study. From the breast US database, a total of 1036 breast US examinations were performed between September 2016 and December 2019 in our institution.

Main points

- Larger size and a non-circumscribed margin are positive axillary lymph node (ALN) predictors on conventional ultrasound (US).
- Distortion of vessels and enhancement range are important predictive factors for ALNs on contrast-enhanced US (CEUS).
- Combining conventional US and CEUS can help predict positive ALNs.

Subjects and lesions

We searched our breast imaging US report database for findings classified as BI-RADS category 4, regardless of clinical data or additional imaging studies. These detections were performed by L.C.Y. owing to more than 20 years of experience in breast US. Patients were included if one or more suspicious lesions were considered as BI-RADS category 4. Patients were excluded if (1) their lesions manifested as non-mass-like types, which mainly refers to the ductal hypoechoic area, non-ductal hypoechoic area, a vague area of altered echotexture with associated architectural distortion and indistinct hypoechoic area with associated posterior acoustic shadowing; (2) their pathologic results were benign; (3) their lesions underwent radiotherapy and chemotherapy before US examination; (4) they did not undergo any pathologic evaluation or adequate location correspondence between their US findings and the pathologic description in our online database; (5) they had not performed any US and CEUS examination; and (6) they had been multifocal on the US.

The reviewers found 944 suspicious lesions in 840 patients. Among them, 36 lesions did not have available pathologic results, 85 were confirmed to be benign, 20 could not accord certain location with the final pathology, 95 showed non-mass-like lesions, 26 underwent radiotherapy and chemotherapy, 430 lacked CEUS results, and 12 showed more than one lesion. These lesions detailed above were excluded from the study. Finally, our study group comprised of 240 lesions, which were subjected to conventional US and CEUS. The diagram of the selection of the study population is shown in Figure 1.

Conventional ultrasound and CEUS on primary tumors

US equipment (MyLab, Twice, ESAOTE S.p.A. Italy) with a linear 4–13 MHz probe (LA523) was introduced for routine US examination, and the images of each lesion were recorded in at least two coordinate planes. Deviations in the description and evaluation of the US images were prevented by employing a single professional doctor (C.Y.L.) who had more than 20 years of experience in breast US. The doctor was blinded to other imaging examinations, such as mammography and magnetic resonance imaging. A junior doctor recorded the reports. The US features of grayscale were described according to the ACR US-BI-RADS standard descriptors.[19] The classifications of color Doppler[20,21] and strain elastography[22-24] are presented in the form of figures (Figures 2, 3). Masses with characteristics such as growth not parallel to the skin or posterior echo attenuation were considered minor suspicion. Intermediate suspicion was defined as having a rich blood supply accompanied by a peak systolic velocity (PSV) of ≥20 cm/s or resistance index (RI) of ≥0.7 or having high elasticity scores (scores 4 and 5) or strain ratio characteristics. Masses with irregular morphology, non-circumscribed margins, or inner microcalcification characteristics were defined as significant suspicion. Lesions with minor findings associated with one intermediate descriptor were classified as BI-RADS category 4A. Lesions with one significant and one minor or intermediate characteristic or two intermediate characteristics were considered BI-RADS 4B. Lesions with one significant and at least two intermediate suspicious findings or two significant suspicious findings were considered BI-RADS 4C.

After a grayscale US examination, CEUS was performed in a timely manner by using an US system (MyLab Twice, ESAOTE S.p.A., Italy) at 3–9 MHz linear probe (LA522) frequencies. CEUS examination was also performed by C.Y.L. Low mechanical index values were applied (<0.2) to reduce the destruction of the contrast agent. The microbubbles (SonoVue™ BRACCO Imaging, S.p.A, Milan, Italy) that were used as a contrast agent were reconstituted with 5 mL of saline (NaCl 0.9%). The contrast agent with 2.4 mL of SonoVue was injected intravenously into an elbow vein according to the manufacturer's instructions at the start of the built-in timer of the US instrument. The US contrast process was continuously recorded in the original data format into the hard disk of the instrument instantly. The enhanced morphological features were then analyzed, and the quantitative parameters of the lesions and normal tissues were assessed with quantification software (QontraXt, AMID and Bracco, Milan, Italy) on the basis of a region of interest over the maximum signal intensity zones. The contrast enhancement pattern of the lesion and the migration and distribution of microbubbles was observed dynamically. The enhancement degree of the lesion was com-

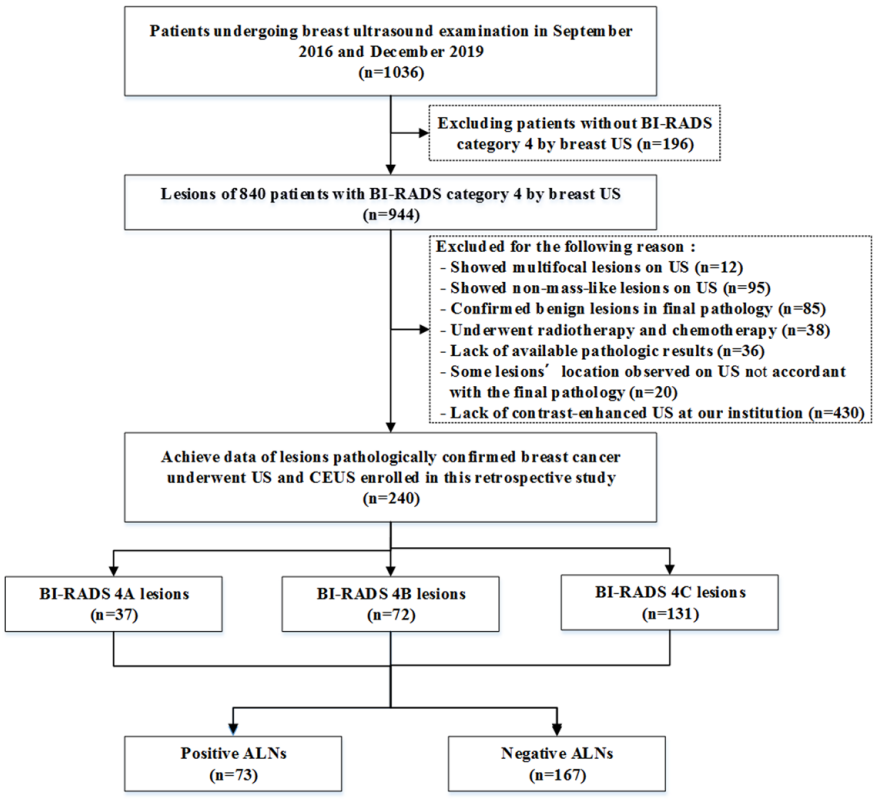

Figure 1. Flowchart illustrating the selection of the study population. US, ultrasound; CEUS, contrast-enhanced US; ALN, axillary lymph node; BI-RADS, Breast Imaging Reporting and Data System.

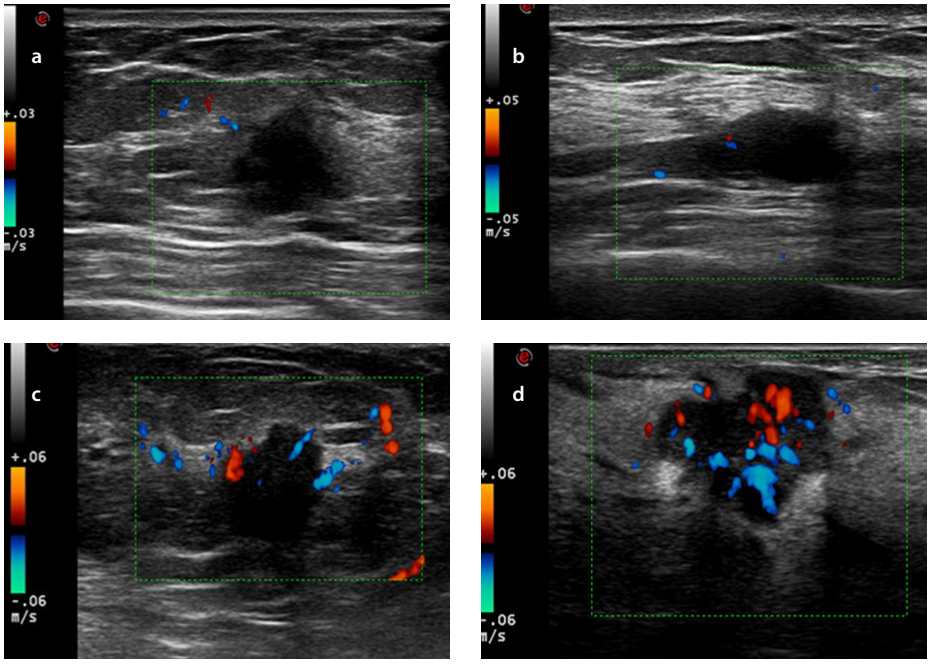

Figure 2. Images of Adler blood flow classification: **(a)** grade 0 mapped no color flow signals in the solid breast mass; **(b)** grade I revealed minimal blood flow signals and mapped punctate color flow; **(c)** grade II revealed moderate blood flow signals and mapped more punctate color flow than grade I or visualized one thick vessel (the diameter of the largest vessel was between 2 and 3 mm) penetrating through the solid breast mass; **(d)** grade III revealed marked blood flow signals and mapped more punctate color flow than grade II or visualized equal or more than two thick vessels interwoven with each other in the solid breast mass.

pared with that of the surrounding breast tissue, including no or iso-enhancement, hypo-enhancement, medium or moderate enhancement, and hyperenhancement.[25,26] Enhancement patterns were characterized as entire or segmental, punctate, linear, or rim enhancements after the administration of the contrast medium.[27] Lesion boundaries were characterized as clear or blurred if most of its circumference (>50%) was clearly or poorly visible after contrast agent administration, respectively. Enhancement morphology was defined as regular or irregular. The presence or absence of perfusion defects and radial penetrating vessels depended on the surrounding tissue toward the lesion. The enhancement order of the lesion was as follows: centripetal enhancement was defined as enhancement from the lesion's periphery towards its center; centrifugal enhancement was defined as beginning from the lesion's center towards its periphery; and diffusion enhancement was manifested as enhancement simultaneously deriving between the lesion's periphery and center.[28] The time-intensity curve (TIC) was defined as slow-in and slow-out, slow-in and fast-out, fast-in and slow-out, and fast-in and fast-out according to the tracing pattern. The quantitative parameters derived from the TIC included: (a) peak intensity (%) calculated by the fraction [(postcontrast intensity–precontrast intensity)/precontrast intensity] × 100%; (b) time to peak (s) defined as the time that elapses between the moment when the contrast medium first reaches the lesion and the time of maximum signal intensity after contrast medium administration; (c) enhancement range was defined as a lesion extent enlarged compared with the conventional US; (d) enhancement area as ≥50% or <50%; and (e) area under the curve (AUC) the TIC.

Model development and classification

The multivariable regression analysis with forward elimination was performed with variables that had *P* values of less than 0.050 on univariate analysis, and three scenario models were developed: (1) model A (conventional US features); (2) model B (CEUS features); and (3) model C (model A plus model B). Receiver operating characteristic (ROC) curves were used to evaluate the discriminatory efficiency of the models. The comparison of the models was assessed using the DeLong test.

Statistical analysis

The data analyzed included the age of the subjects, lesion size, stratification derived from US imaging characteristics (BI-RADS category 4A, 4B, or 4C), CEUS characteristics, and categorized pathologic results. Statistical analysis was conducted using the software packages SPSS v25.0 and MedCalc v12.7. Continuous data were compared with the independent t-test as appropriate, and variables with abnormal or non-normal distribution were analyzed by the Mann–Whitney U test. Categorical variables were compared using Fisher's exact test or the Pearson chi-square test. Then, multivariate logistic regression analyses were introduced to determine the most valuable variables for identifying positive LNs through conventional US and CEUS. Multiple ROC curves were drawn to illustrate and compare the value of identified risk variables in the prediction of a positive LN. ALN prediction capacity was assessed by the AUC, sensitivity, and specificity, and the comparison of the models was evaluated using the DeLong test. A *P* value of <0.05 was considered to illustrate a statistically significant difference.

Results

A detailed list of lesion descriptors stratified in accordance with the estimated malignancy risk in BI-RADS category 4 is shown in Table 1. The most common breast cancer in this study was infiltrative ductal carcinoma, which was found in 183 of 240 malignant patients (76.1%), followed by ductal carcinoma in situ in 34 of 240 patients (14.2%). Increased histological grades of 2 or 3 and positive ALN rates were found in BI-RADS 4C, then 4B, and lastly, 4A. Table 2 shows the age, pathological types, histological grades, and positive LN results in groups 4A, 4B, and 4C.

Univariate analyses are presented in Table 3 regarding the US and CEUS descriptors for predicting positive LNs. In the conventional US features, the univariate analyses showed that lesion size, margin, blood flow, PSV, RI, posterior echo, and BI-RADS category were associated with positive ALNs ($P < 0.05$). In the CEUS features, vessel perforation or distortion, enhancement range, and TIC curves were significantly different between positive and negative groups ($P < 0.05$). Among the multivariate analyses (Table 4), lesion size [odds ratio (OR), 1.11; 95% confidence interval (CI), 1.06–1.64], margin (OR, 3.39; 95% CI, 1.75–6.57), perforation or distortion vessels (OR, 3.94; 95% CI, 2.04–7.63), and enhancement range (OR, 0.28; 95% CI, 0.15–0.55) were the most important factors to distinguish positive ALNs ($P <0.001$). These imaging features of the tumor are shown in Figures 4 and 5. The ROC curves (Figure 6) showed that model C yielded the better AUC of 0.82 (95% CI, 0.75–0.88) than model A (AUC, 0.74; 95% CI, 0.68–0.81) and model B (AUC, 0.72; 95% CI, 0.65–0.80). Model C yielded optimal diagnostic performance in predicting positive ALN compared with the other two models (both $P < 0.05$, as per the DeLong test). The sensitivity of model A, B, and C were 67.1%, 41.1%, and 80.8%, respectively, while the specificity was 73.1%, 92.2%, and 72.9%, respectively.

Discussion

The present study identified that the traits of larger size and non-circumscribed margin are marked as two independent predictors for positive ALNs on conventional US. We also found that vessel perforation or distortion and a conspicuous TIC curve are the other two important predictive factors for positive ALNs on CEUS. ROC curve comparison showed that the performance of the combined conventional US and CEUS is better than the performance of each alone. On conventional US, an excellent relationship was established between the primary tumor size and the prevalence of positive ALNs in this study. Sopik and Narod[29] demonstrated there was a clear linear correlation between tumor size and metastasis for breast cancers about 7 and 60 mm in size. Akissue de Camargo Teixeira et al.[30] agreed that tumor size could be taken as a traditional predictor of ALN status. The average pre-surgical tumor size was 3.3 ± 2.1 cm in patients with LN metastasis and 2.5 ± 1.4 cm in patients without metastasis.[30] These findings are consistent with our results. Cancer cells inside the tumor spread, survive, and then pervade to regional LNs and further to other distant sites.[31] Therefore, more cancer cells are available in a larger-sized tumor to metastasize. Tseng et al.[32] proved that tumor size was closely relevant to lymphovascular invasion, which was confirmed to be the standard of LN metastasis pathology and consequently closely connected with positive ALNs. In this study, invasive ductal carcinoma also dominated, which indicated the remarkable significance of the maximum diameter of the tumor in predicting positive ALNs.

In addition, the non-circumscribed margin was identically correlated with positive ALNs. Costantini et al.[33] pointed out that sonographic signs, such as margin burrs and angular and microlobulated margins, are important factors for biological behaviors associated with metastatic pervasion. The unevenness of the tumor margin indicates a high possibility of invasive growth with a malignant tendency. In breast cancer with high aggressiveness and tumor burden, carcinoma cells can infiltrate the surrounding tissues, lymphatic vessels, and blood vessels at different growth speeds, resulting in a non-smooth tumor margin.[17]

Through CEUS examination, we found that vessel perforation or distortion is important to the prediction of positive ALNs. A malignant tumor has vascular contortions because its blood vessels cannot maintain their regular shapes during the rapid growth of the lesions.[12] Santamaría et al.[34] demonstrated that tumor arteries detected by color Doppler and sonographic tumor size were an independent predictor of ALN status. Yu et al.[35] demonstrated that perforating vessels are also a risk factor of LN metastasis in patients suffering from small breast cancer. These findings almost matched our results showing that vessel perforation or distortion is strongly linked with positive ALNs in patients with small breast cancer (maximum diameter ≤2.0 cm) and also bounded with breast carcinoma in the T2 stage (2.0 cm < maximum diameter ≤5.0 cm) dominating in this study. This finding could explain why large tumors with abundant blood supply are usually accompanied by thick vessels.

Furthermore, this study also discovered the perfusion pattern of the fast-in and fast-out pattern as the only quantitative parameter for identifying positive ALNs with a significant difference. This finding was consistent with the report of Wang et al.[36], which revealed that the perfusion performance of the peripheral region of breast cancer is characterized by hyperechoic enhancement and fast-in and fast-out patterns. The shape of the dynamic enhancement curve is related to the microscopic characteristics of the main components of poorly differentiated tumors, which are scattered malignant vascular endothelial cells.[37,38] The lack of capillary networks and incomplete cavities resulted in the rapid flushing of the contrast agent. Such features thereby influence the ALN status through the hemodynamic principle.[39]

Regarding the correlation between qualitative and quantitative CEUS characteristics and pathological prognostic factors in patients with breast cancer, Vraka et al.[27] suggested that the qualitative assessment of the enhancement pattern is better than quantitative assessment for differentiating malig-

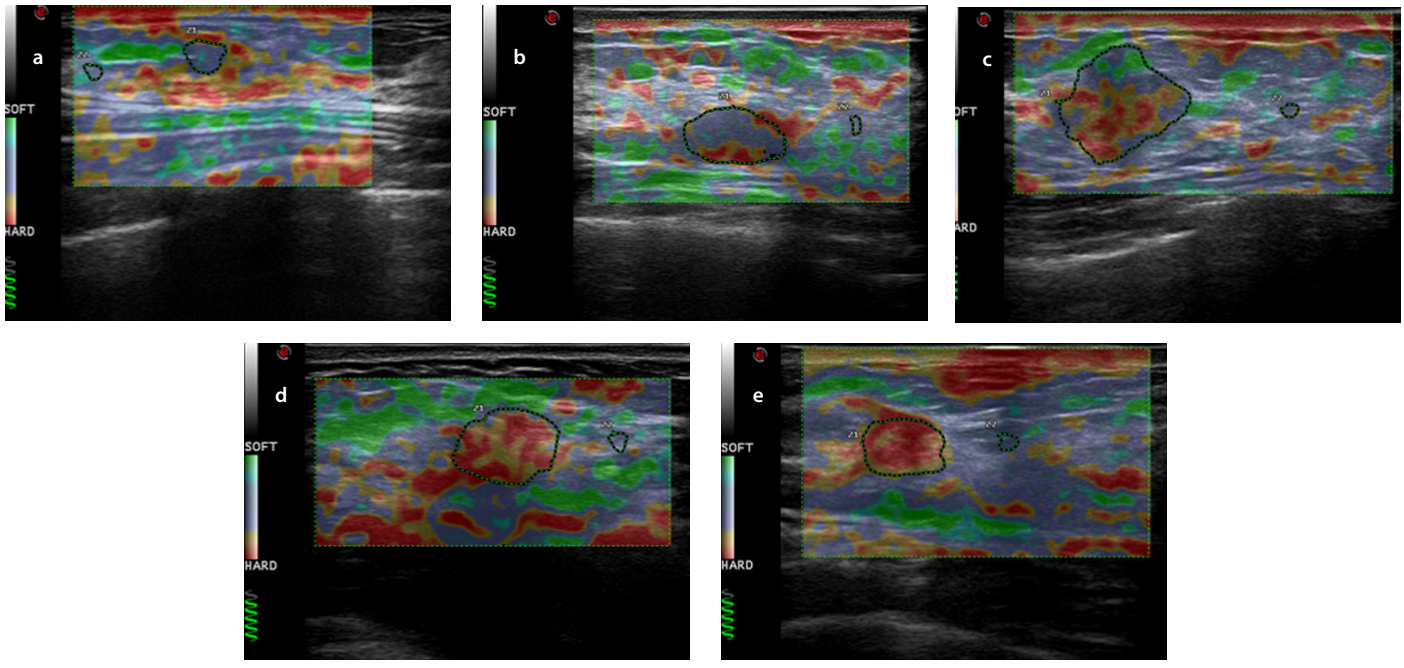

Figure 3. Images of elasticity classification: **(a)** score 1: the entire lesion or nearly the entire lesion was green, and the elastic strain ratio was <2.5; **(b)** score 2: the focus was red in the center and homogeneous elasticity in the periphery, and the elastic strain ratio was <2.5; **(c)** score 3: the proportions of green and red in the range of lesion were the same, and the elastic strain ratio was <2.5; **(d)** score 4: the entire lesion was red or little green was found inside the lesion, and the elastic strain ratio was ≥2.5; (e) score 5: the lesion and surrounding tissues were all shown in red, with or without green in the inner part, and the elastic strain ratio was far beyond 2.5.

Table 1. Lesion descriptors stratified in accordance with the estimated malignancy risk

Minor	Intermediate	Major
Non-parallel to skin	Adler blood flow grade: 2 or 3	Larger tumor size
Posterior echo attenuation	PSV ≥20 cm/s	Irregular shape
	RI ≥0.7	Non-circumscribed margin
	Elastic score: 4 or 5	Microcalcification
	Elastic strain ratio: ≥2.5	

PSV, peak systolic velocity; RI, resistance index.

Table 2. Source of clinical and pathological materials

BI-RADS	4A	4B	4C
Age	49.55 ± 11.89	49.38 ± 11.53	51.73 ± 11.67
Pathology types			
Invasive ductal carcinoma	17 (7.2%)	50 (20.9%)	115 (48.0%)
Ductal carcinoma *in situ*	12 (5.0%)	13 (5.4%)	9 (3.8%)
Mucinous carcinoma	5 (2.1%)	4 (1.7%)	3 (1.3%)
Papillary carcinoma	3 (1.1%)	4 (1.5%)	1 (0.4%)
Others	1 (0.4%)	2 (0.8%)	1 (0.4%)
Histological grades			
1	3 (1.4%)	2 (0.9%)	3 (1.2%)
2	14 (5.8%)	34 (14.1%)	60 (24.9%)
3	16 (6.8%)	36 (14.8%)	53 (22.1%)
Unknown	19 (8.0%)		
ALNs			
Negative	33 (13.8%)	53 (22.0%)	81 (33.8%)
Positive	4 (1.7%)	19 (7.9%)	50 (20.8%)

ALN, axillary lymph node; BI-RADS, Breast Imaging Reporting and Data System.

Table 3. Univariate analysis of conventional ultrasound, elastography, and CEUS for the prediction of positive ALNs in BI-RADS category 4 lesions

Descriptors		Negative ALNs (n = 167), n (%)	Positive ALNs (n = 73), n (%)	*P* value
Conventional US plus elastography				
Size (mm)		21.21 ± 7.19	25.78 ± 5.83	<0.001*
Shape	Regular	49 (29.3)	19 (26.0)	0.600
	Irregular	118 (70.7)	54 (74.0)	
Margin	Circumscribed	80 (47.9)	18 (24.7)	0.001*
	Non-circumscribed	87 (52.1)	55 (75.3)	
Orientation	Parallel	88 (52.7)	35 (47.9)	0.498
	Non-parallel	79 (47.3)	38 (52.1)	
Posterior echo	Unaltered or enhanced	157 (94.0)	63 (86.3)	0.047*
	Attenuation	10 (6.0)	10 (13.7)	
Micro-calcification	Without	124 (74.3)	59 (80.8)	0.271
	With	43 (25.7)	14 (19.2)	
RI	<0.7	94 (56.3)	30 (41.1)	0.030*
	≥0.7	73 (43.7)	43 (58.9)	
Elastic	Score 1–2	18 (10.8)	7 (9.6)	0.920
	Score 3–4	133 (79.6)	58 (79.5)	
	Score 5	16 (9.6)	8 (10.9)	
Adler blood flow	Grade 0–I	47 (28.1)	15 (20.5)	0.216
	Grade II–III	120 (71.9)	58 (79.5)	
BI-RADS category	4A	33 (19.8)	4 (5.5)	0.004*
	4B	53 (31.7)	19 (26.0)	
	4C	81 (48.5)	50 (68.5)	
PSV (cm/s)		11.86 ±3.46	12.94 ± 4.08	0.036*
Elastic strain ratio		2.15 ± 0.38	2.10 ± 0.34	0.362
Contrast-enhanced US				
Enhancement boundary	Distinct	86 (51.5)	40 (54.8)	0.638
	Indistinct	81 (48.5)	33 (45.2)	
Enhancement morphology	Regular	41 (24.6)	18 (24.7)	0.986
	Irregular	126 (81.4)	55 (75.3)	
Enhancement degree	Iso- or no enhancement	8 (4.8)	2 (2.7)	0.622
	Hypo-enhancement	19 (11.4)	10 (13.7)	
	Moderate enhancement	10 (6.0)	7 (9.6)	
	Hyper-enhancement	130 (77.8)	54 (74.0)	
Enhancement pattern	Entire	100 (59.9)	47 (63.4)	0.348
	Segmental	39 (23.3)	19 (26.0)	
	Others	28 (16.8)	7 (9.6)	
Enhancement order	Centripetal	129 (77.2)	55 (75.3)	0.955
	Centrifugal	34 (20.4)	16 (21.9)	
	Diffuse	4 (2.4)	2 (2.7)	
Perfusion defects	Without	97 (58.1)	35 (47.9)	0.146
	With	70 (41.9)	38 (52.1)	
Perforation or distortion vessels	Without With	116 (69.5) 51 (30.5)	27 (37.0) 46 (63.0)	<0.001*

Table 3. Continues

Descriptors		Negative ALNs (n = 167), n (%)	Positive ALNs (n = 73), n (%)	*P* value
Enhancement area	<50%	24 (14.4)	12 (16.4)	0.680
	≥50%	143 (85.6)	61 (83.6)	
Enhancement range	None	111 (66.5)	28 (38.4)	<0.001*
	Enlarged	56 (33.5)	45 (61.6)	
Peak intensity	-	50.35 ± 3.49	50.96 ± 3.77	0.229
TTP	-	56.27 ± 6.43	57.06 ± 6.71	0.396
AUC	-	5.14 ± 3.05	5.24 ± 2.40	0.793
TIC curve	Slow-in and slow-out	71 (42.5)	19 (26.0)	<0.001*
	Slow-in and fast-out	29 (17.4)	5 (6.9)	
	Fast-in and slow-out	46 (27.5)	12 (16.4)	
	Fast-in and fast-out	21 (12.6)	37 (50.7)	

P value is derived from the univariate association analyses between each of the variables and ALN status. **P* value of <0.05. ALN, axillary lymph node; PSV, peak systolic velocity; RI, resistance index; TTP, time to peak; AUC, area under the curve; TIC, time-intensity curve; BI-RADS, Breast Imaging Reporting and Data System; CEUS, contrast-enhanced ultrasound.

Table 4. Multivariate analysis of the comparison between conventional ultrasound and CEUS for predicting positive ALNs in BI-RADS category 4 lesions

Characteristics	Odds ratio	95% confidence Interval	*P* value
Size	1.110	1.061–1.161	<0.001
Margin			
Circumscribed	Reference		
Non-circumscribed	3.393	1.752–6.570	<0.001
Perforation or distortion vessels			
Without	Reference		
With	3.941	2.037–7.625	<0.001
Enhancement range			
None	Reference		
Enlarged	0.283	0.146–0.550	<0.001
TIC curve			
Slow-in and slow-out	Reference		
Slow-in and fast-out	0.741	0.239–2.301	0.604
Fast-in and slow-out	1.222	0.507–2.942	0.655
Fast-in and fast-out	7.092	3.142–16.010	<0.001

TIC, time-intensity curve; CEUS, contrast-enhanced ultrasound; ALN, axillary lymph node; BI-RADS, Breast Imaging Reporting and Data System.

nant lesions. Wang et al.[40] also demonstrated that qualitative parameters significantly improve the performance of CEUS in the distinction of benign and malignant breast lesions, which is clinically promising. Our study showed similar results and demonstrated the positive role of CEUS, especially its qualitative parameters, for the differentiation of positive ALNs in BI-RADS category 4 malignant breast lesions. The superiority of qualitative CEUS parameters lies in the fact that the reviewer's experience could rectify probable technological errors, which could not be achieved in quantitative parameters. In addition, some uncontrolled factors, such as patient respiration movements and a preselected interest area by the CEUS performer, can impact the quantitative parameters' evaluation of the received images during video recording. Meanwhile, quantitative parameters were created by an offline workstation, which is another technological restriction. Thus, further studies regarding more advanced equipment and optimized software need to be performed in this field to improve the accuracy of CEUS.

Three predictive models based on conventional US features (model A), CEUS features (model B), and the combined model A + B (model C) were then constructed and compared. Model C illustrated significant improvement in diagnostic accuracy and model fit in predicting positive ALNs. The multivariate-based combination model can be extracted to reveal tumor microvascular imaging and to evaluate the comprehensive characterization of underlying malignant tumor signs. This model plays a potential role in avoiding subject diagnosis. Tumors with nodal metastasis have completely different grayscale ultrasonic, color Doppler, and internal construction enhancement characteristics. The four best-performing combination features were tumor size, margin, vessel perforation or distortion, and TIC curve. Discriminating positive ALNs by using a single sonography factor is difficult. The incorpora-

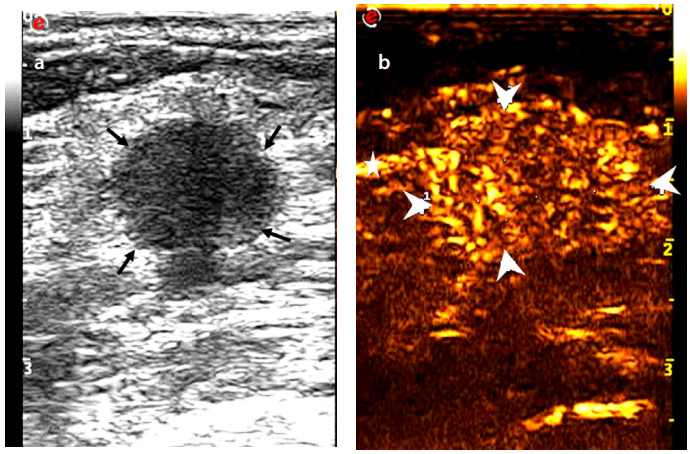

Figure 4. Images of a 53-year-old female diagnosed with invasive ductal carcinoma in the right breast: **(a)** tumor with a maximum diameter of 1.7 cm showed a circumscribed margin on the conventional ultrasound (thin arrow), and no suspicious axillary lymph node was observed; **(b)** tumor with an extended range of 2.1 cm showed an unclear boundary (thick arrow) and vessel perforation entering from surrounding tissue into the mass (fine arrow). One-node macrometastasis was found in the final pathological results.

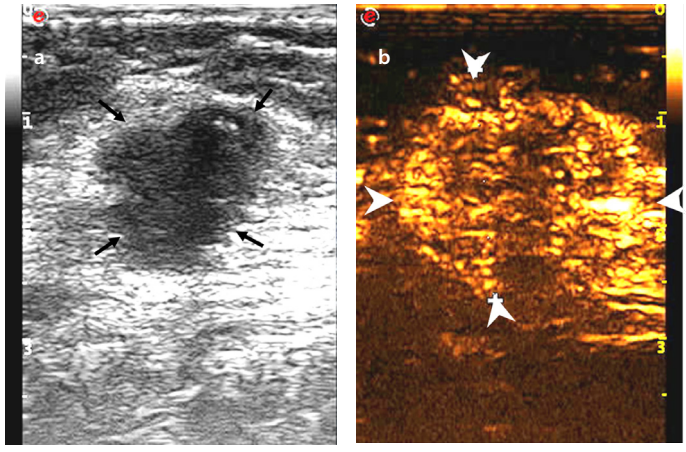

Figure 5. Images of a 55-year-old female diagnosed with invasive ductal carcinoma in the right breast: **(a)** tumor with a maximum diameter of 2.0 cm showed a non-circumscribed margin on the conventional ultrasound (thin arrow), and no suspicious axillary lymph node was present; **(b)** tumor with an extended range of 2.6 cm showed a clear boundary, and vessel perforation (thick arrow) in surrounding tissue or mass was absent. Non-node metastasis was found in the final pathological results.

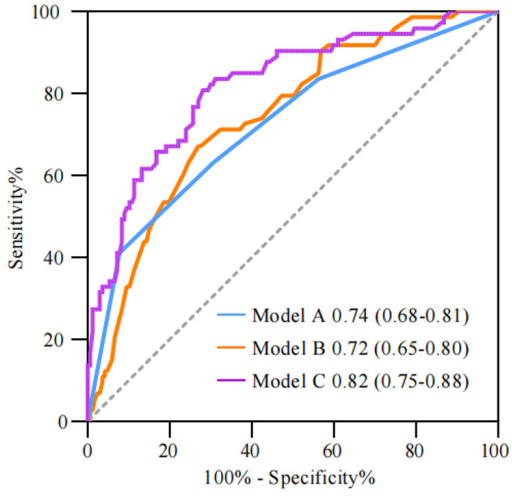

Figure 6. Receiver operating characteristic curves using the three different diagnostic models of differentiating non-metastatic and metastatic groups: model A, conventional ultrasound (US) model; model B, contrast-enhanced US (CEUS model; model C, conventional US plus CEUS model.

tion of multiple factors can provide a comprehensive and robust approach. The multivariate-based combination model, which can discriminate positive ALNs from negative ones, showed significant improvement compared with models A or B alone.

We acknowledge several limitations of our study. First, patient selection bias may exist because of its retrospective nature. Second, the data applied in our study are from a single institution. Thus, our findings lack a general and robust assessment. Therefore, a rigorous analysis should be planned with data from a larger number of patients collected from more institutions in different areas. Third, the external validation of different races or populations was absent because of the relatively small single sample size of CEUS. Fourth, intra- and inter-observer reliability was not evaluated in this study.

In conclusion, the combination of conventional US and CEUS could facilitate increasing diagnostic performance during the prediction of positive ALNs in BI-RADS category 4 breast cancer lesions. Therefore, our predictive model may also facilitate clinical decision making and potentially improve the diagnostic performance of the selected patients.

Conflict of interest disclosure

The authors declared no conflicts of interest.

References

1. Elverici E, Barça AN, Aktaş H, et al. Nonpalpable BI-RADS 4 breast lesions: sonographic findings and pathology correlation. *Diagn Interv Radiol.* 2015;21(3):189-194. [CrossRef]
2. Hong AS, Rosen EL, Soo MS, Baker JA. BI-RADS for sonography: positive and negative predictive values of sonographic features. *AJR Am J Roentgenol.* 2005;184(4):1260-1265. [CrossRef]
3. Heinig J, Witteler R, Schmitz R, Kiesel L, Steinhard J. Accuracy of classification of breast ultrasound findings based on criteria used for BI-RADS. *Ultrasound Obstet Gynecol.* 2008;32(4):573-578. [CrossRef]
4. Magny SJ, Shikhman R, Keppke AL. Breast Imaging Reporting and Data System. StatPearls. Treasure Island (FL): StatPearls Publishing Copyright© 2021, StatPearls Publishing LLC., 2021. [CrossRef]
5. Spinelli Varella MA, Teixeira da Cruz J, Rauber A, Varella IS, Fleck JF, Moreira LF. Role of BI-RADS Ultrasound Subcategories 4A to 4C in Predicting Breast Cancer. *Clin Breast Cancer.* 2018;18(4):507-511. [CrossRef]

6. Sedgwick EL, Ebuoma L, Hamame A, et al. BI-RADS update for breast cancer caregivers. *Breast Cancer Res Treat.* 2015;150(2):243-254. [CrossRef]
7. Ouyang Q, Chen L, Zhao H, Xu R, Lin Q. Detecting metastasis of lymph nodes and predicting aggressiveness in patients with breast carcinomas. *J Ultrasound Med.* 2010;29(3):343-352. [CrossRef]
8. Rubaltelli L, Beltrame V, Scagliori E, et al. Potential use of contrast-enhanced ultrasound (CEUS) in the detection of metastatic superficial lymph nodes in melanoma patients. *Ultraschall Med.* 2014;35(1):67-71. [CrossRef]
9. Saracco A, Szabó BK, Aspelin P, et al. Differentiation between benign and malignant breast tumors using kinetic features of real-time harmonic contrast-enhanced ultrasound. *Acta Radiol.* 2012;53(4):382-388. [CrossRef]
10. Liu H, Jiang YX, Liu JB, Zhu QL, Sun Q, Chang XY. Contrast-enhanced breast ultrasonography: Imaging features with histopathologic correlation. *J Ultrasound Med.* 2009;28(7):911-920. [CrossRef]
11. Balleyguier C, Opolon P, Mathieu MC, et al. New potential and applications of contrast-enhanced ultrasound of the breast: own investigations and review of the literature. *Eur J Radiol.* 2009;69(1):14-23. [CrossRef]
12. Wan CF, Du J, Fang H, Li FH, Zhu JS, Liu Q. Enhancement patterns and parameters of breast cancers at contrast-enhanced US: correlation with prognostic factors. *Radiology.* 2012;262(2):450-459. [CrossRef]
13. Zhang JX, Cai LS, Chen L, Dai JL, Song GH. CEUS helps to rerate small breast tumors of BI-RADS category 3 and category 4. *Biomed Res Int.* 2014;2014:572532. [CrossRef]
14. Li Q, Hu M, Chen Z, et al. Meta-analysis: contrast-enhanced ultrasound versus conventional ultrasound for differentiation of benign and malignant breast lesions. *Ultrasound Med Biol*. 2018;44(5):919-929. [CrossRef]
15. Xiao X, Dong L, Jiang Q, Guan X, Wu H, Luo B. Incorporating contrast-enhanced ultrasound into the bi-rads scoring system improves accuracy in breast tumor diagnosis: a preliminary study in China. *Ultrasound Med* Biol. 2016;42(11):2630-2638. [CrossRef]
16. Ansari B, Morton MJ, Adamczyk DL, et al. Distance of breast cancer from the skin and nipple impacts axillary nodal metastases. *Ann Surg Oncol*. 2011;18(11):3174-3180. [CrossRef]
17. Bae MS, Shin SU, Song SE, Ryu HS, Han W, Moon WK. Association between US features of primary tumor and axillary lymph node metastasis in patients with clinical T1-T2N0 breast cancer. *Acta Radiol*. 2018;59(4):402-408. [CrossRef]
18. Zhou LQ, Wu XL, Huang SY, et al. Lymph node metastasis prediction from primary breast cancer US images using deep learning. *Radiology*. 2020;294(1):19-28. [CrossRef]
19. Berg WA, Cosgrove DO, Doré CJ, et al. Shear-wave elastography improves the specificity of breast US: the BE1 multinational study of 939 masses. *Radiology*. 2012;262(2):435-449. [CrossRef]
20. Adler DD, Carson PL, Rubin JM, Quinn-Reid D. Doppler ultrasound color flow imaging in the study of breast cancer: preliminary findings. *Ultrasound Med Biol*. 1990;16(6):553-559. [CrossRef]
21. Ecanow JS, Abe H, Newstead GM, Ecanow DB, Jeske JM. Axillary staging of breast cancer: what the radiologist should know. *Radiographics*. 2013;33(6):1589-1612. [CrossRef]
22. Youk JH, Son EJ, Kim JA, Gweon HM. Pre-operative evaluation of axillary lymph node status in patients with suspected breast cancer using shear wave elastography. *Ultrasound Med Biol*. 2017;43(8):1581-1586. [CrossRef]
23. Itoh A, Ueno E, Tohno E, et al. Breast disease: clinical application of US elastography for diagnosis. *Radiology*. 2006;239(2):341-350. [CrossRef]
24. Kanagaraju V, Dhivya B, Devanand B, Maheswaran V. Utility of ultrasound strain elastography to differentiate benign from malignant lesions of the breast. *J Med Ultrasound*. 2021;29(2):89-93. [CrossRef]
25. Wan C, Du J, Fang H, Li F, Wang L. Evaluation of breast lesions by contrast enhanced ultrasound: qualitative and quantitative analysis. Eur J Radiol. 2012;81(4):444-450. [CrossRef]
26. Du LW, Liu HL, Gong HY, et al. Adding contrast-enhanced ultrasound markers to conventional axillary ultrasound improves specificity for predicting axillary lymph node metastasis in patients with breast cancer. *Br J Radiol*. 2021;94(1118):20200874. [CrossRef]
27. Vraka I, Panourgias E, Sifakis E, et al. Correlation between contrast-enhanced ultrasound characteristics (qualitative and quantitative) and pathological prognostic factors in breast cancer. *In Vivo*. 2018;32(4):945-954. [CrossRef]
28. Leng X, Huang G, Ma F, Yao L. Regional contrast-enhanced ultrasonography (CEUS) characteristics of breast cancer and correlation with microvessel density (MVD). *Med Sci Monit*. 2017;23:3428-3436. [CrossRef]
29. Sopik V, Narod SA. The relationship between tumour size, nodal status and distant metastases: on the origins of breast cancer. *Breast Cancer Res Treat*. 2018;170:647-656. [CrossRef]
30. Akissue de Camargo Teixeira P, Chala LF, Shimizu C, et al. Axillary lymph node sonographic features and breast tumor characteristics as predictors of malignancy: a nomogram to predict risk. *Ultrasound Med Biol*. 2017; 43:1837-1845. [CrossRef]
31. Boughey JC, Ballman KV, Hunt KK, et al. Axillary ultrasound after neoadjuvant chemotherapy and its impact on sentinel lymph node surgery: results from the American College of Surgeons Oncology Group Z1071 Trial (Alliance). *J Clin Oncol*. 2015;33(30):3386-3393. [CrossRef]
32. Tseng HS, Chen LS, Kuo SJ, Chen ST, Wang YF, Chen DR. Tumor characteristics of breast cancer in predicting axillary lymph node metastasis. *Med Sci Monit*. 2014;20:1155-1161. [CrossRef]
33. Costantini M, Belli P, Ierardi C, Franceschini G, La Torre G, Bonomo L. Solid breast mass characterisation: use of the sonographic BI-RADS classification. *Radiol Med*. 2007;112(6):877-894. [CrossRef]
34. Santamaría G, Velasco M, Farré X, Vanrell JA, Cardesa A, Fernández PL. Power Doppler sonography of invasive breast carcinoma: does tumor vascularization contribute to prediction of axillary status? *Radiology*. 2005;234(2):374-380. [CrossRef]
35. Yu X, Hao X, Wan J, Wang Y, Yu L, Liu B. Correlation between ultrasound appearance of small breast cancer and axillary lymph node metastasis. *Ultrasound Med Biol.* 2018;44(2):342-349. [CrossRef]
36. Wang X, Xu P, Wang Y, Grant EG. Contrast-enhanced ultrasonographic findings of different histopathologic types of breast cancer. *Acta Radiol.* 2011;52:248-255. [CrossRef]
37. Metz S, Daldrup-Unk HE, Richter T, et al. Detection and quantification of breast tumor necrosis with MR imaging: value of the necrosis-avid contrast agent gadophrin-3. *Acad Radiol.* 2003;10(5):484-490. [CrossRef]
38. Colpaert C, Vermeulen P, van Beest P, et al. Intratumoral hypoxia resulting in the presence of a fibrotic focus is an independent predictor of early distant relapse in lymph node-negative breast cancer patients. *Histopathology.* 2001;39(4):416-425. [CrossRef]
39. Teifke A, Behr O, Schmidt M, et al. Dynamic MR imaging of breast lesions: correlation with microvessel distribution pattern and histologic characteristics of prognosis. *Radiology.* 2006;239(2):351-360. [CrossRef]
40. Wang Y, Fan W, Zhao S, et al. Qualitative, quantitative and combination score systems in differential diagnosis of breast lesions by contrast-enhanced ultrasound. *Eur J Radiol.* 2016;85(1):48-54. [CrossRef]